Journal of Theoretical Biology 570 (2023) 111521

Contents lists available at ScienceDirect

Journal of Theoretical Biology

journal homepage: www.elsevier.com/locate/yjtbi

What explains the poor contraction of the viral load during paediatric HIV infection?

Juliane Schröter *, Rob J. de Boer

Theoretical Biology & Bioinformatics, Utrecht University, Utrecht, The Netherlands

ARTICLE INFO

Keywords:
Virus–host dynamics
Viral replication rate
Peak over setpoint viral load ratio
Mathematical modelling
Parameter sweep

ABSTRACT

An acute HIV infection in young children differs markedly from that in adults: Children have higher viral loads (VL), and a poor contraction to a setpoint VL that is not much lower than the peak VL. As a result, children progress faster towards AIDS in the absence of treatment. We used a classical ordinary differential equation model for viral infection dynamics to study why children have a lower viral contraction ratio than adults. We performed parameter sweeps to identify factors explaining the observed difference between children and adults. We grouped parameters associated with the host, the infection, or the immune response. Based on paediatric data available from datasets within the EPIICAL project (https://www.epiical.org/), we refuted that viral replication rates differ between young children and adults, and therefore these cannot be responsible for the low VL contraction ratios seen in children. The major differences in lowering VL contraction ratio resulted from sweeping the parameters linked to the immune response. Thus, we postulate that an "ineffective" (late and/or weak) immune response is the most parsimonious explanation for the higher setpoint VL in young children, and hence the reason for their fast disease progression.

1. Introduction

Several mathematical models describe the course of an acute HIV infection in adults by very similar mechanisms, i.e., by classical within-host viral kinetics (Ho et al., 1995; Wei et al., 1995; Perelson et al., 1996; Kirschner and Webb, 1996; Nowak et al., 1997; de Boer and Perelson, 1998; Nowak and May, 2000; Stafford et al., 2000; Perelson, 2002; Canini and Perelson, 2014; van Dorp et al., 2020). HIV infects CD4+ T-cells and replicates rapidly, as indicated by a steep initial increase of the viral load (VL), peaking around 10^6 RNA copies/mL within a few weeks, and is accompanied by a progressive loss of CD4+ T-cells (Kaufmann et al., 1998; Little et al., 1999). Once the target cells decline and the immune response is mobilised, the viral load declines several orders of magnitude (10–100 fold) to a setpoint VL within a few months [Kaufmann1998, Richardson2003]. The CD4+ T-cell population recovers and a "quasi" steady state is attained, that is maintained for years to decades until acquired immunodeficiency syndrome (AIDS) develops (Babiker et al., 2000).

An acute paediatric HIV infection course looks very different from the one in adults. Children can acquire HIV before birth (during pregnancy) or at birth (Tobin and Aldrovandi, 2013). In the first case they are typically born with a high viral load. In the second case, the initial phase during which the VL increases is often not observed because this phase is short and data is sparse (De Rossi et al., 1996). Some data sets suggest that peak VL levels in infants can be up to 10 fold higher compared to adults during an acute HIV infection (Shearer et al., 1997; Biggar et al., 2001; Richardson et al., 2003). After reaching the peak, the VL hardly contracts in young children, and high VLs are typically maintained (McIntosh et al., 1996; Richardson et al., 2003; Goulder et al., 2016). As a consequence, an untreated paediatric HIV infection typically progresses fast, AIDS develops within 1 year, and children often do not survive their second birthday without treatment (Goulder et al., 2016).

In the literature several reasons can be found to explain these observed differences in VLs between adult and paediatric acute HIV infections. (i) A high VL peak may result from fast viral replication (De Rossi et al., 1996). (ii) HIV-targeted CD4+ T-cell densities might be higher in children compared to adults (Bonhoeffer et al., 2003). Due to a shift in the T-cell compartment from naive towards memory T-cells, (iii) the virus tropism in a primary paediatric HIV infection might be different (Davenport et al., 2002; Ribeiro et al., 2006), or (iv) different target cell subpopulations might be infected (Essunger and Perelson, 1994). (v) A poor viral contraction might be explained by the immature state of immune system of children, which makes them more susceptible to infections in general (De Rossi et al., 1996; Tobin and Aldrovandi, 2013; Goulder et al., 2016).

The aim of this study is to find mechanistic explanations of why children have a lower viral contraction compared to adults. Using a

* Correspondence to: Padualaan 8, 3584 CH Utrecht, NL, The Netherlands.
E-mail address: schj.work@gmail.com (J. Schröter).

https://doi.org/10.1016/j.jtbi.2023.111521
Received 26 July 2022; Received in revised form 3 February 2023; Accepted 30 April 2023
Available online 9 May 2023

conventional mathematical model for viral infection, we performed parameter sweeps to test which parameter differences between adults and children account for the observed differences in the course of an acute HIV infection. We thereby identify individual parameter settings accounting for the low contraction observed in children, while the peak VL remained unchanged. Whenever possible, we incorporate paediatric data from the EPIICAL project (https://www.epiical.org/) to validate parameters.

2. Methods

2.1. Data

Longitudinal measurements from untreated HIV-positive infants are rare, particularly during the initial phase of the infection, which only last a few weeks. We were able to select HIV RNA measurements of 7 HIV-positive children from European Pregnancy and Paediatric Infections Cohort Collaboration (EPPICC) – a study that was designed to study early antiretroviral treatment initiations (EPPICC, 2011). The selected measurements were taken within 14 days after birth and before treatment initiation. We required at least 2 valid HIV RNA measurements per child fulfilling these conditions. A valid measurement was defined as detectable HIV RNA with an explicit VL. We excluded measurements at the detection limits. These measurements are considered to be taken at early time points during an acute HIV infection.

2.2. Viral replication rate

For each of these 7 children, the initial viral growth rate, ρ, has been calculated by using linear regression on the natural logarithmic-transformed VL measurements, i.e.:

$$\rho = \frac{ln[V(t_2)] - ln[V(t_1)]}{t_2 - t_1}, \tag{1}$$

where $V(t_1)$ and $V(t_2)$ are two measurements at the two early time points t_1 and t_2. Similar to Ribeiro et al. (2010), we used Eq. (1) to estimate the viral replication rate in children.

2.3. Acute HIV infection model

This study is based on a conventional model for an acute HIV infection with a target population T, early infected cells I_1, late infected cells I_2, and immune effector cells E (like cytotoxic T cells or NK cells) (Gadhamsetty et al., 2016; van Dorp et al., 2020). As the dynamics of the virus V are much faster than those of the infected cells, a (conventional) quasi steady state assumption applies for the viral population, implying that V is proportional to I_2, i.e., $V = cI_2$. The remainder of the model is defined in terms of ordinary differential equations (ODE), i.e.:

$$\frac{dT}{dt} = \sigma - d_T T - \beta T I_2, \tag{2}$$

$$\frac{dI_1}{dt} = f\beta T I_2 - (d_T + \gamma)I_1 - k_1 I_1 nE, \tag{3}$$

$$\frac{dI_2}{dt} = \gamma I_1 - (d_T + \alpha)I_2 - k_2 I_2 nE, \tag{4}$$

$$\frac{dE}{dt} = p_E \frac{EI_2}{h + E + I_2} - d_E E. \tag{5}$$

Target cells, T, which can consist of CD4+ T-cells and other CD4+ cell types like macrophages, are produced at a constant rate σ, and have a death rate d_T. They are infected by virus produced by infected cells, I_2, with an infection rate β. Following Gadhamsetty et al. (2016) we derive an expression for how the initial replication rate, ρ, depends on all parameters of the model (2)–(5), by linearisation around the uninfected steady state (i.e., for $T = \frac{\sigma}{d_T}$ and $E = 0$). Subsequently, one can solve the infection rate, β, from this expression to estimate the unknown infection rate from the other parameters, including the known initial replication rate, i.e.,

$$\beta = \frac{(d_T + \gamma + \rho)(d_T + \alpha + \rho)}{f\gamma \overline{T}}, \text{ with } \overline{T} = \frac{\sigma}{d_T}.$$

If not otherwise stated we fixed β to 4.2×10^{-5}, which corresponds to a replication rate of $\rho = 1/\text{day}$.

Only a fraction f of T cells infected by HIV turns into successfully infected cells I_1 (Doitsh et al., 2014). After some time, called the eclipse-phase, here with an average length of $1/\gamma$ days, these cells turn into virus producing cells I_2 (Dixit et al., 2004). I_1 and I_2 die at their natural death rate d_T, while productively infected cells I_2 are also affected by the virus-induced cytopathic effects, α (Markowitz et al., 2003). Several clones of cytotoxic effector cells (n) kill I_1 cells at a rate k_1, and I_2 cells at a rate k_2 respectively. Note that the n and k_i cannot be separated in this model and are treated as two parameter combinations nk_1 and nk_2. The division rate of immune effector cells E increases as a function of the viral load. This is implemented using a competitive saturation term defining a maximum division rate, p_E, and a saturation constant h. Effector cells E have a death rate d_E.

Models like this (2)–(5) have three steady states (de Boer and Perelson, 1998): (1) in the absence of infection $T = \frac{\sigma}{d_T}$ and $I_1 = I_2 = E = 0$; (2) in the absence of an immune response, $E = 0$, there is a 'target cell limited' steady state of the infection; and (3) in the presence of an immune response, $E > 0$, there exists an 'immune-controlled' steady state of the infection.

The implementation of the model and the analyses were performed in R. We make use of a wrapper grind.R around the FME package for simulations of the infection course (Soetaert and Petzoldt, 2010).

Table 1
Default parameter values for acute HIV infection in adults. The parameters correspond mainly to those of van Dorp et al. (2020).

Parameter	Value	Units	Explanation
σ	10^5	cells mL^{-1} day^{-1}	Source of target cells
d_T	0.1	day^{-1}	Death rate of target cells
β	4.2×10^{-5}	cells^{-1} mL day^{-1}	Infection rate
f	0.1	–	Fraction of non-abortive infected cells
$1/\gamma$	1.0	day	Eclipse time
α	0.9	day^{-1}	Virus-induced cytopathic effect
$n \times k_1$	0	cells^{-1} mL day^{-1}	Killing rate of early-infected cells
$n \times k_2$	10^{-4}	cells^{-1} mL day^{-1}	Killing rate of virus-producing cells
p_E	1.1	day^{-1}	Maximal division rate of effector cells
d_E	0.1	day^{-1}	Death rate of effector cells
h	10^4	cells mL^{-1}	Saturation constant
c	45	–	Scaling parameter for viral load
ρ	1	day^{-1}	Viral replication rate

3. Results

3.1. Acute adult HIV dynamics as default

With the parameters presented in Table 1, the mathematical model (2)–(5) describes a typical acute HIV infection course in adults (Fig. 1). We initiated the model with $T(0) = 10^6$ target cells/mL, which refers to the homeostatic level, $\overline{T}$, in the infection-free state. An infection was introduced by one infected cell ($I_1(0) = 1$). The initial value for the effector cells was set to $E(0) = 0.1$ cells/mL to allow for the expected delay of a few weeks in immune responses to a viral infection. The model was simulated for 365 days which is longer than the typical time taken to reach the setpoint VL after an acute HIV infection in adults. The viral load increases steeply, peaks and then declines towards a plateau. The decline is stepwise towards the setpoint VL. The first drop in the VL is due to target cell limitation and the second is induced by the onset of the immune response (de Boer and Perelson, 1998), which here occurs after the VL peak. The setpoint VL plateau is established by 3 months and is, in our example, around 10-fold lower than the peak

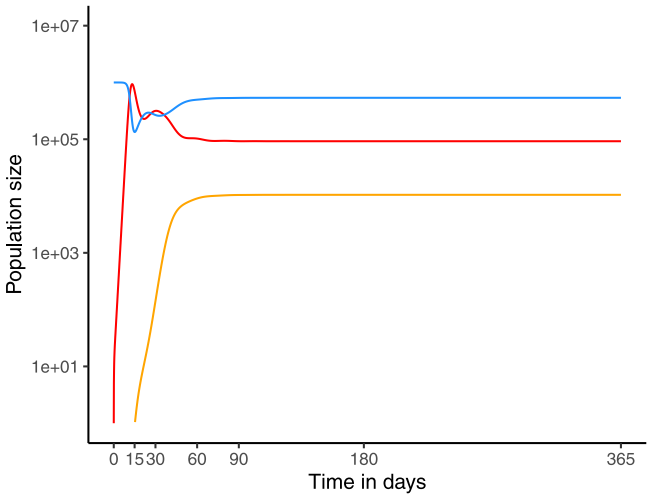

Fig. 1. Trajectory of an acute HIV infection in adults. The course of the target cell population T (blue), the virus population V (red) and the effector population E (yellow) are presented. At the start of infection the target cell population is at its homeostatic level ($T(0) = 10^6$ cells mL^{-1}). Infection is introduced with 1 infected cell ($I_1(0) = 1$, $I_2(0) = 0$). Effector cells are delayed by setting the initial effector population to $E(0) = 0.1$.

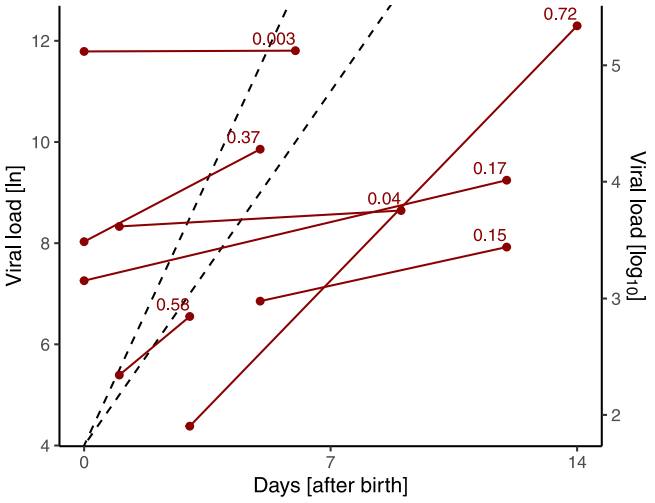

Fig. 2. Viral replication rates in children. For 7 children untreated viral loads measured within the first 2 weeks after birth are shown, and compared to the viral replication rates of adults. Measurements (red bullets) per child are connected by a solid line. The second measurement is labelled with the estimated initial growth rate estimated by Eq. (1). Adult replication rates of 1 and 1.5 per day are illustrated by the slopes of the dashed black lines (Little et al., 1999; Ribeiro et al., 2010).

value. The actual fold difference between peak and setpoint VL depends on various parameters, including the killing rate $n \times k_2$, which illustrates that adults with a broader set of cellular immune responses ($n > 1$) are expected to have a lower setpoint VL (Edwards et al., 2002; Kiepiela et al., 2007). The here described dynamics of an acute HIV infection in adults (Fig. 1) serve as a default and the 10 fold change between peak and setpoint VL as a benchmark to evaluate differences in the ratio of VL contraction.

3.2. Paediatric viral replication rate comparable to adults

The high VLs in children have been attributed to faster viral replication rates than observed in adults (Bonhoeffer et al., 2003). We estimated the viral replication rate by calculating the initial growth rate from VL measurements taken from 7 untreated children (Fig. 2). Estimating the replication rate from Eq. (1), we find a median viral growth rate of 0.17/day (IQR = [0.01, 0.48]). In these children, paediatric viral replications rates appear to be slower than those of adults which are reported to be between 1 and 1.5 per day (Little et al., 1999; Ribeiro et al., 2010). Although, we have only included measurements taken within the first 2 weeks after birth, we may have missed (part of) the initial growth phase since HIV infection can have occurred in utero. However, in most children the VL increases, suggesting that peak VL has not been reached and that we do capture (most of) the initial expansion phase (Fig. 2). Hence, we have no evidence that paediatric viral replication rates are faster compared to those in adults.

3.3. Parameter sweeps to understand poor VL contraction ratio in children

Based on the 'adult' acute HIV infection model (2)–(5), we took a "non-supervised" approach to investigate how different parameter settings in children could explain their poor contraction from peak to setpoint VL. We refer to this from now on as the contraction ratio, i.e., the ratio of the peak over the setpoint VL (peak/setpoint VL), which is typically high in adults and low in infants. By grouping the parameters into host-, infection- and immune-associated, we searched for parameters that markedly affect the contraction ratio. Changing one parameter at a time, we keep the remaining ones at their default values as listed in Table 1; this is mainly for reasons of simplicity. The contraction ratio can change because either the peak VL and/or the setpoint VL change. We are mostly interested in explaining heightened setpoint VLs, i.e., low viral contraction ratios, because peak VLs tend to be high in children. We therefore scan all parameters of the model to test whether or not changing them can deliver this feature, i.e., a decreasing contraction ratio with a similar peak VL. We find that some parameters do and others cannot. The parameters that can would be able to account for this major difference between children and adults. The setpoint viral load is reported for two scenarios in the absence of any immune response ("target cell limited", dashed lines) and in the presence of an immune response ("immune controlled", solid lines in Figs. 3 and 5). Both scenarios result in a steady state of the VL.

3.3.1. Simultaneous changes in source and death rate of target cells result in lower VL contraction ratios

First we investigated the host-associated parameters (Fig. 3). An adult acute HIV infection typically starts at the homeostatic state, $T(0) = \sigma/d_T$, of the CD4+ target cells. The immune system of children is immature and developing, i.e. the target cell numbers need not be in steady state. By perturbing the number of initial target cells, we mimic an immune system that is not yet in homeostasis. An increased initial $T(0)$ resulted in an increased peak VL but (obviously) had no effect on the setpoint VL. Thus, changes in ratio between the peak and setpoint VL are mainly caused by changes in peak VL (Fig. 3A).

Assuming a homeostatic state of the target cell population before infection, and decreasing the source term σ (Fig. 3B), or increasing the death rate d_T (Fig. 3C) decreases the contraction ratio. However, this was also mainly due to changes in the peak VLs. Interestingly, by increasing the death rate of the target cell population in the absence of changing the initial values (i.e. changing the source and death rate simultaneously, Fig. 3D) a slightly smaller contraction ratio can be achieved, that is mainly due to an increase in the setpoint VL, while peak VL remains constant. This was mostly visible in the target cell regulated steady state, i.e., in the absence of an immune response, however.

3.3.2. Non-cytopathic virus can damp the VL contraction ratio

Second, we investigated the infection-associated parameters (Fig. 4). We perturbed the infection rate (β, Fig. 4A), the fraction of successfully infected cells (f, Fig. 4B), duration of eclipse phase (γ, Fig. 4C), and the virus-induced cytopathic effect (α, Fig. 4D). Decreasing the

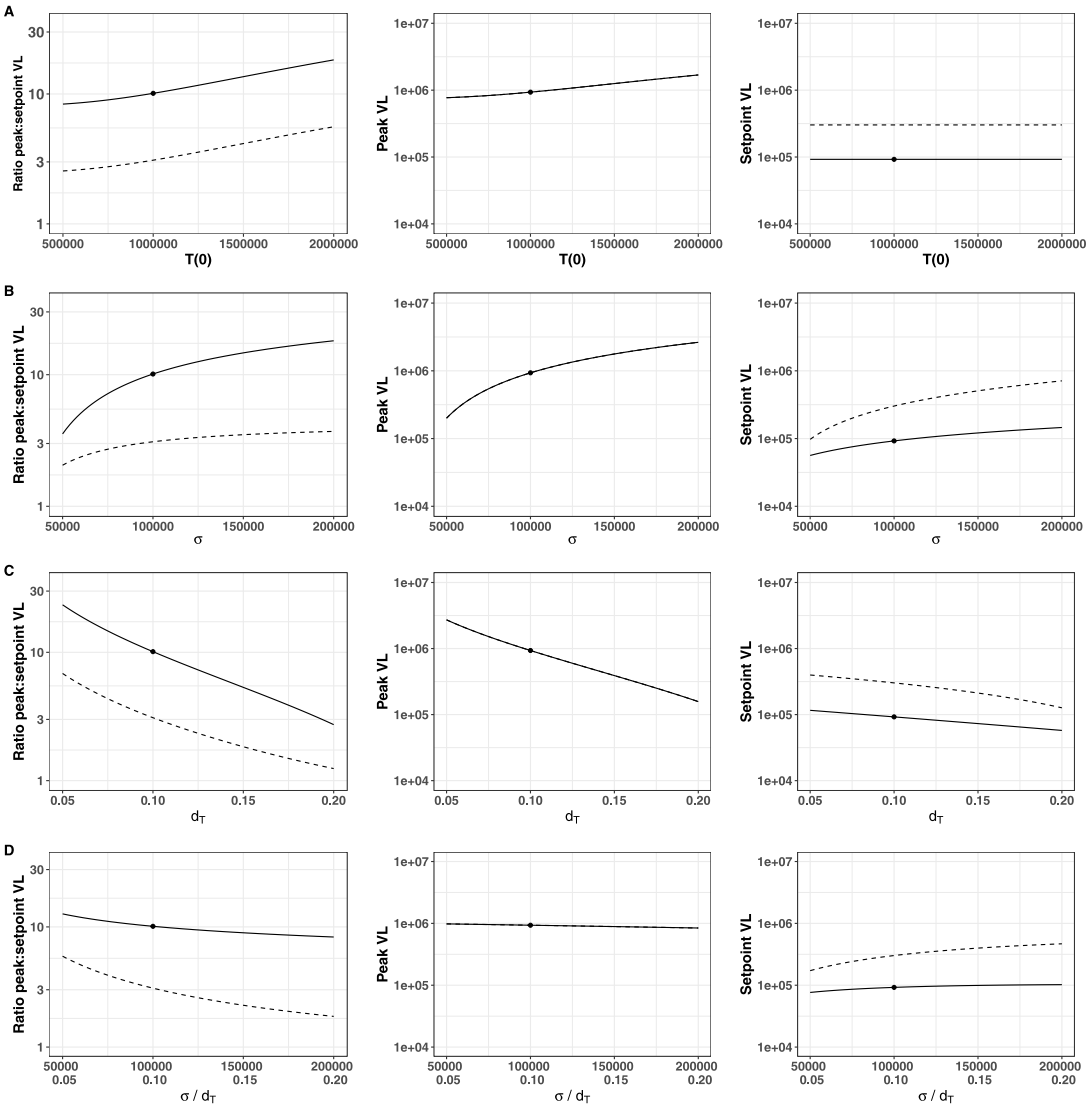

Fig. 3. Effect of host-associated parameters. The effect of the changes in (A) initial target cell population, $T(0)$, (B) source of target cells, σ, (C) death rate of the target cell population, d_T, and (D) σ and d_T simultaneously to maintain the same initial values $T(0) = 10^6$, on the ratio peak:setpoint VL (left panels), the peak VL (middle panels) and the setpoint value taken at day 365 (right panels) are illustrated. Parameters are changed individually and the remaining parameters are kept at the default values in Table 1. An exception is panel (D), in which σ and d_T are changed simultaneously. Bullets represent the default values. The solid lines represent the immune-controlled state and the dashed lines the target cell limited steady state. Since the peak VL is largely determined by target cell availability in our model, both lines overlap in the middle panels.

parameters β and γ reduces the VL contraction ratio, but this was once again mainly caused by a decline in the peak VL. The setpoint level itself hardly changed (Fig. 4A/C). The setpoint VL slightly increases by increasing the fraction of cells becoming infected (f), but this had almost no effect on the VL contraction ratio – at least not in the absence of any immune response – as peak values increased simultaneously (Fig. 4B). Decreasing the cytopathicity α resulted in increased setpoint viral loads. While in the immune-controlled scenario the contraction ratio increased, the target cell limited scenario showed the opposite effect, and the VL contraction ratio decreased, despite the same peak VLs (Fig. 4D). A virus with almost no cytopathic effect of the virus dampens the contraction ratio towards one in the absence of an immune response.

3.3.3. Immune response is the most parsimonious explanation for poor VL contraction

Finally, we investigated the parameters associated with the immune response (Fig. 5). As already seen in Figs. 3 and 4, the absence of immune responses (target cell limited scenario, $E = 0$) had a dominant influence on the contraction ratio. Changes in the parameters associated with the immune response confirmed these observations. A lower division rate (p_E, Fig. 5A), a higher sensitivity to recognise antigens (h, Fig. 5B), a reduced killing rate or fewer numbers of effector cells ($n \times k_2$, Fig. 5C), as well as a shorter expected life time of the effector cells (d_E, Fig. 5D) led all to a reduced ratio between peak and setpoint VL. As peak values remained similar, the lower contraction ratio was mainly due to the increase in setpoint VLs. Thus, reduced immune responses in children appear to be the most parsimonious explanation for a low contraction ratio in VL.

4. Discussion and conclusion

An acute HIV infection in children is known to be very different from that in adults, as children tend to have a high VL and do not show the typical contraction towards a markedly lower setpoint VL (Richardson et al., 2003; Goulder et al., 2016). Via parameter sweeps in an viral infection model, we here showed that the low contraction ratio in children is readily explained by an immature state of their cellular immune response, and not easily by any other factors. A higher death

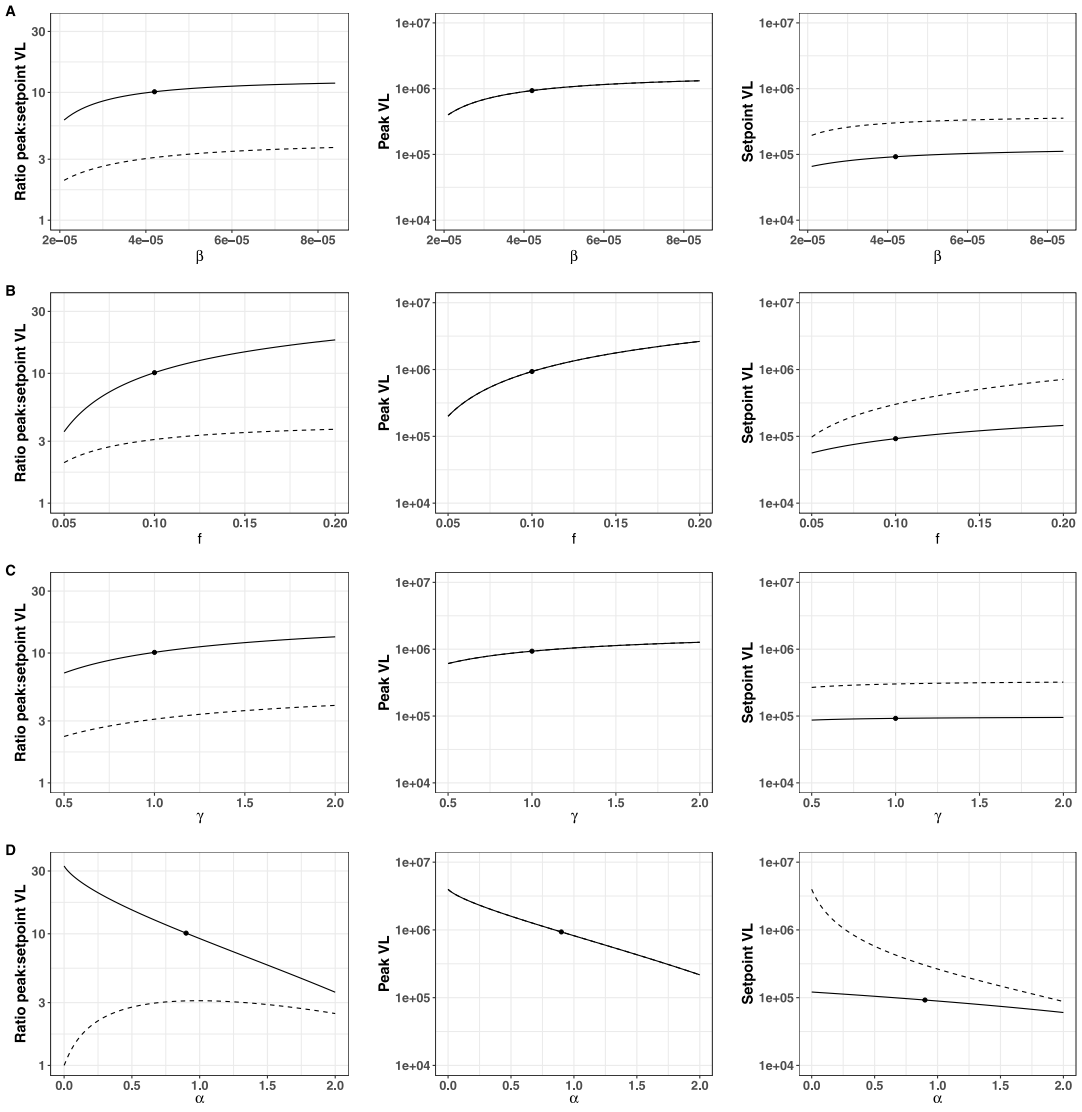

Fig. 4. Effect of infection-associated parameters. The effect of changes in (A) infection rate (β), (B) fraction of successfully infected cells (f), (C) duration of eclipse phase (γ), and (D) virus-induced cytopathic effect (α) on the ratio peak:setpoint VL (left panels), the peak VL (middle panels) and the setpoint value taken at day 365 (right panels) are illustrated. Parameters are changed individually and the remaining parameters are set to the default values in Table 1. The bullets represent the default values. The solid lines represent the immune-controlled state and the dashed lines the target cell limited steady state. Since the peak VL is largely determined by target cell availability in our model, both lines overlap in the middle panels.

rate of the target cell population in the absence of changing the initial value of the target cells, as well as lower cytopathic effects of the virus, also reduce the contraction ratio without increasing peak VLs, but only in the absence of an immune response. We therefore identify a poor early immune response as the most parsimonious factor explaining the poor contraction that is typically observed in paediatric HIV infection.

High setpoint VLs have been postulated to be due to high viral replication rates (De Rossi et al., 1996). We were unable to confirm that the viral replication rate is faster in children compared to adults. The initial HIV viral growth rate in adults has been estimated to be 1–1.5 per day (Little et al., 1999; Ribeiro et al., 2010), which is similar to that during an SIV infection in macaques (Nowak et al., 1997). By calculating the initial viral growth rate of 7 untreated children, we could not find any evidence for higher viral replication rates compared to adults. We are limited to only a few infants in our dataset, and that maternal HIV treatment might affect our results (explaining the slow viral replication rates), but none of the 7 children would support a replication rate higher than 1 per day as observed in adults (Ribeiro et al., 2010). Since pre-ART measurements in children are sparse, it is difficult to improve upon this analysis, and the data provide at least no evidence for the hypothesis that HIV replicates faster in young children. Interestingly, Nagaraja et al. (2021) reports that the reproductive ratio R_0 increases with age in children of 0 to 17 years old. Since this calculation is mainly based on the ratio of CD4 T-cell counts in healthy and HIV-infected children, which is somewhat indirect, we find it difficult to compare this to our more direct measure of viral replication rate. Measurements taken during untreated paediatric HIV infection course will remain rare because most infants who are sampled are also treated. Hence, further insights into natural acute paediatric HIV infections can only be obtained from existing experimental material, or by mathematical modelling. Using the latter, we provide a mechanistic understanding for the poor viral contraction seen in most paediatric HIV infection.

There is ample experimental evidence that the CD8+ cellular immune response plays an important role in controlling HIV infections in adults, and in controlling SIV infections in macaques (McBrien et al., 2018). For instance, a recent study showed that HIV-specific CD8+ T cells become functionally impaired in HIV infected individuals who

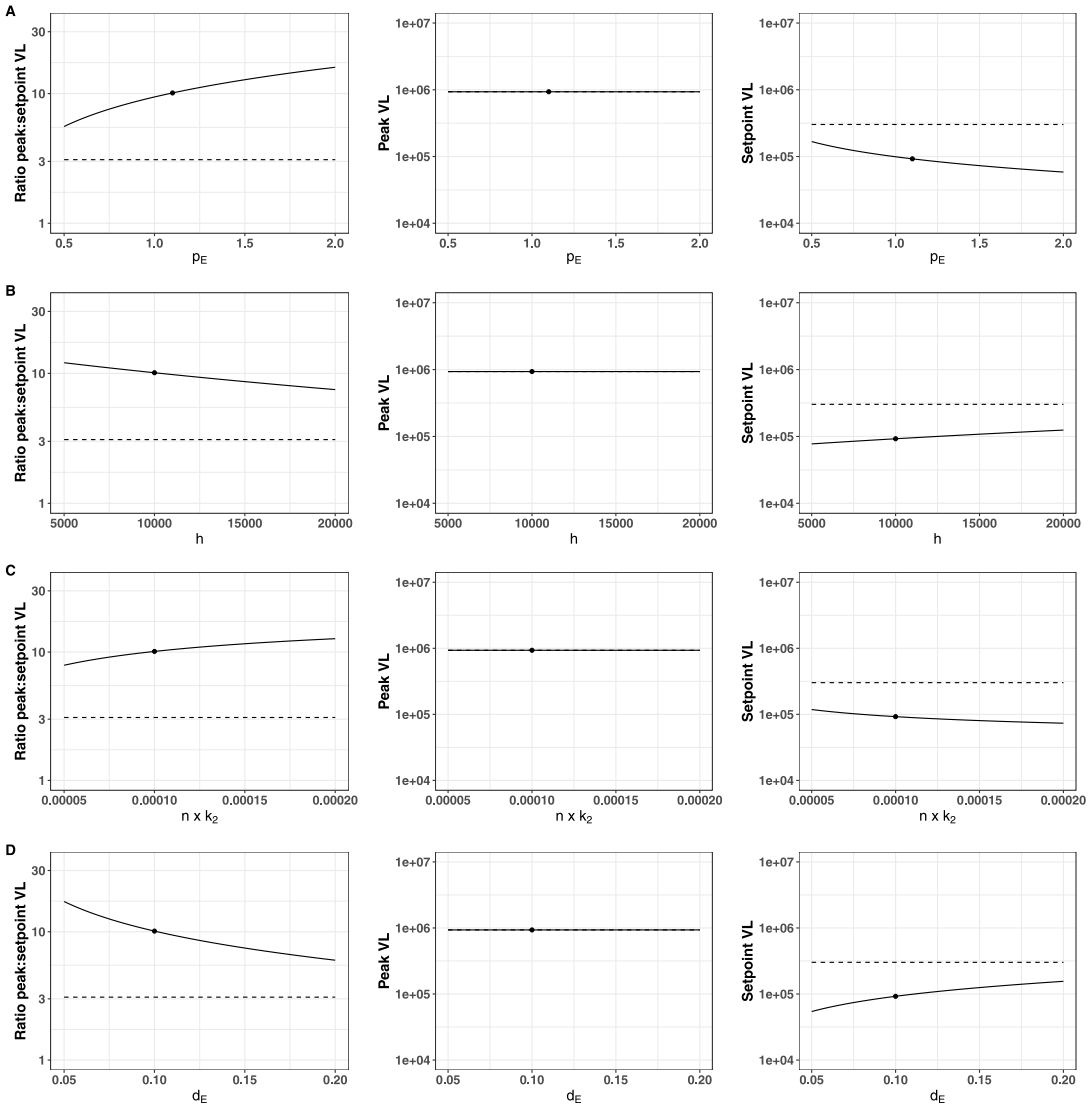

Fig. 5. Effect of immune-associated parameters. The effect of changes in (A) division rate of effector cells (p_E), (B) Michaelis Menten constant (h), (C) killing rate ($n \times k_2$), and (D) death rate of effector cells (d_E) on the ratio peak:setpoint VL (left panels), the peak VL (middle panels) and the setpoint value taken at day 365 (right panels) are illustrated. Parameters are changed individually and the remaining parameters are set to the default values in Table 1. The bullets represent the default values. The solid lines represent the immune-controlled state and the dashed lines the target cell controlled steady state. Since the peak VL is largely determined by target cell availability in our model, both lines overlap in the middle panels.

spontaneously controlled the virus but then show an aborted viral control (Collins et al., 2021). The depletion of CD8+ T cells during acute and chronic SIV infection has a major effect on the viral load (Schmitz et al., 1999; Cardozo et al., 2018). Importantly, there is hardly any contraction of the SIV VL when CD8+ T cells are depleted in the initial phase of the infection (Schmitz et al., 1999), which mimics the poor contraction of the HIV VL that is typically observed in children. Moreover, it is typically hard to find HIV-specific immune responses in young children living with HIV (Palma et al., 2015). Also for other viruses like CMV, influenza, and RSV, it is known that very young children show poor immune responses. Indeed, the VL contraction ratio is increased in somewhat older children that become infected with HIV (Richardson et al., 2003). These observations are in good agreement with our postulate that the poor VL contraction ratio in paediatric HIV infection is due to a late and/or poor immune response.

In conclusion, an immature cellular immune response in infants readily explains their poor control of an early HIV infection. As a high setpoint VL is a strong predictor for fast disease progression, this also explains why untreated infants progress fast towards AIDS, and why it is important to control the virus as fast as possible.

CRediT authorship contribution statement

Juliane Schröter: Conceptualization, Formal analysis, Visualization, Writing – original draft. **Rob J. de Boer:** Conceptualization, Supervision, Writing – review & editing.

Declaration of competing interest

None

Acknowledgements

We would like to thank EPPICC for their support in allocating the data and our colleagues Peter de Greef and Arpit Swain for their critical reading and their suggestions for improvement of the manuscript.

Funding

JS was partly funded by Utrecht University, Netherlands and the EPIICAL project (funded through an independent grant by ViiV Healthcare United Kingdom).

References

Babiker, A., Darby, S., De Angelis, D., Ewart, D., Porter, K., Beral, V., Darbyshire, J., Day, N., Gill, N., 2000. Time from HIV-1 seroconversion to AIDS and death before widespread use of highly-active antiretroviral therapy: a collaborative re-analysis. Lancet 355 (9210), 1131–1137.

Biggar, R.J., Broadhead, R., Janes, M., Kumwenda, N., Taha, T.E.T., Cassol, S., 2001. Viral levels in newborn African infants undergoing primary HIV-1 infection. AIDS 15 (10), 1311–1313.

Bonhoeffer, S., Funk, G.A., Günthard, H.F., Fischer, M., Müller, V., 2003. Glancing behind virus load variation in HIV-1 infection. TIM 11 (11), 499–504.

Canini, L., Perelson, A.S., 2014. Viral kinetic modeling: State of the art. J. Pharmacokinet. Pharmacodyn. 41 (5), 431.

Cardozo, E.F., Apetrei, C., Pandrea, I., Ribeiro, R.M., 2018. The dynamics of simian immunodeficiency virus (SIV) after depletion of CD8+ cells. Immunol. Rev. 285 (1), 26.

Collins, D.R., Urbach, J.M., Racenet, Z.J., Arshad, U., Power, K.A., Newman, R.M., Mylvaganam, G.H., Ly, N.L., Lian, X., Rull, A., Rassadkina, Y., Yanez, A.G., Peluso, M.J., Deeks, S.G., Vidal, F., Lichterfeld, M., Yu, X.G., Gaiha, G.D., Allen, T.M., Walker, B.D., 2021. Functional impairment of HIV-specific CD8 + T cells precedes aborted spontaneous control of viremia. Immunity 54 (10), 2372–2384.e7.

Davenport, M.P., Zaunders, J.J., Hazenberg, M.D., Schuitemaker, H., Van Rij, R.P., 2002. Cell turnover and cell tropism in HIV-1 infection. TIM 10 (6), 275–278.

de Boer, R.J., Perelson, A.S., 1998. Target cell limited and immune control models of HIV infection: A comparison. J. Theoret. Biol. 190 (3), 201–214.

De Rossi, A., Masiero, S., Giaquinto, C., Ruga, E., Comar, M., Giacca, M., Chieco-Bianchi, L., 1996. Dynamics of viral replication in infants with vertically acquired human immunodeficiency virus type 1 infection. J. Clin. Investig. 97 (2), 323–330.

Dixit, N.M., Markowitz, M., Ho, D.D., Perelson, A.S., 2004. Estimates of intracellular delay and average drug efficacy from viral load data of HIV-infected individuals under antiretroviral therapy. Antivir. Ther. 9 (2), 237–246.

Doitsh, G., Galloway, N.L., Geng, X., Yang, Z., Monroe, K.M., Zepeda, O., Hunt, P.W., Hatano, H., Sowinski, S., Muñoz-Arias, I., Greene, W.C., 2014. Cell death by pyroptosis drives CD4 T-cell depletion in HIV-1 infection. Nature 505 (7484), 509–514.

Edwards, B.H., Bansal, A., Sabbaj, S., Bakari, J., Mulligan, M.J., Goepfert, P.A., 2002. Magnitude of functional CD8+ T-cell responses to the gag protein of human immunodeficiency virus type 1 correlates inversely with viral load in plasma. J. Virol. 76 (5), 2298–2305.

EPPICC, 2011. Response to early antiretroviral therapy in HIV-1 infected infants in Europe , 1996–2008. AIDS 25 (18), 2279–2287.

Essunger, P., Perelson, A.S., 1994. Modeling HIV infection of CD4+ T-cell subpopulations. J. Theoret. Biol. 170 (4), 367–391.

Gadhamsetty, S., Coorens, T., de Boer, R.J., 2016. Notwithstanding circumstantial alibis, cytotoxic T cells can be major killers of HIV-1-infected cells. J. Virol. 90 (16), 7066–7083.

Goulder, P.J., Lewin, S.R., Leitman, E.M., 2016. Paediatric HIV infection: the potential for cure. Nat. Rev. Immunol. 16 (4), 259–271.

Ho, D.D., Neumann, A.U., Perelson, A.S., Chen, W., Leonard, J.M., Markowitz, M., 1995. Rapid turnover of plasma virions and CD4 lymphocytes in HIV-1 infection. Nature 373 (6510), 123–126.

Kaufmann, G.R., Cunningham, P., Kelleher, A.D., Zaunders, J., Carr, A., Vizzard, J., Law, M., Cooper, D.A., 1998. Patterns of viral dynamics during primary human immunodeficiency virus type 1 infection. J. Infect. Dis. 178 (6), 1812–1815.

Kiepiela, P., Ngumbela, K., Thobakgale, C., Ramduth, D., Honeyborne, I., Moodley, E., Reddy, S., De Pierres, C., Mncube, Z., Mkhwanazi, N., Bishop, K., Van Der Stok, M., Nair, K., Khan, N., Crawford, H., Payne, R., Leslie, A., Prado, J., Prendergast, A., Frater, J., McCarthy, N., Brander, C., Learn, G.H., Nickle, D., Rousseau, C., Coovadia, H., Mullins, J.I., Heckerman, D., Walker, B.D., Goulder, P., 2007. CD8+ T-cell responses to different HIV proteins have discordant associations with viral load. Nat. Med. 13 (1), 46–53.

Kirschner, D., Webb, G.F., 1996. A model for treatment strategy in the chemotherapy of aids. Bull. Math. Biol. 58 (2), 367–390.

Little, S.J., McLean, A.R., Spina, C.A., Richman, D.D., Havlir, D.V., 1999. Viral dynamics of acute HIV-1 infection. J. Exp. Med. 190 (6), 841.

Markowitz, M., Louie, M., Hurley, A., Sun, E., Di Mascio, M., Perelson, A.S., Ho, D.D., 2003. A novel antiviral intervention results in more accurate assessment of human immunodeficiency virus type 1 replication dynamics and T-cell decay in vivo. J. Virol. 77 (8), 5037–5038.

McBrien, J.B., Kumar, N.A., Silvestri, G., 2018. Mechanisms of CD8 + T cell-mediated suppression of HIV/SIV replication. Eur. J. Immunol. 48 (6), 898–914.

McIntosh, K., Ahevitz, A., Zaknun, D., Kornegay, J., Chatis, P., Karthas, N., Burchett, S.K., 1996. Age- and time-related changes in extracellular viral load in children vertically infected by human immunodeficiency virus. Pediatr. Infect. Dis. J. 15.

Nagaraja, P., Gopalan, B.P., D'Souza, R.R., Sarkar, D., Rajnala, N., Dixit, N.M., Shet, A., 2021. The within-host fitness of HIV-1 increases with age in ART-naïve HIV-1 subtype C infected children. Sci. Rep. 11 (1), 1–10.

Nowak, M.A., Lloyd, A.L., Vasquez, G.M., Wiltrout, T.A., Wahl, L.M., Bischofberger, N., Williams, J., Kinter, A., Fauci, A.S., Hirsch, V.M., Lifson, J.D., 1997. Viral dynamics of primary viremia and antiretroviral therapy in simian immunodeficiency virus infection. J. Virol. 71 (10), 7518–7525.

Nowak, M.A., May, R.M., 2000. Virus Dynamics: Mathematical Principles of Immunology and Virology. Oxford University Press, Oxford; New York.

Palma, P., Foster, C., Rojo, P., Zangari, P., Yates, A., Cotugno, N., Klein, N., Luzuriaga, K., Pahwa, S., Nastouli, E., Gibb, D.M., Borkowsky, W., Bernardi, S., Calvez, V., Manno, E., Mora, N., Compagnucci, A., Wahren, B., Muñoz-Fernández, M., De Rossi, A., Ananworanich, J., Pillay, D., Giaquinto, C., Rossi, P., 2015. The EPIICAL project: an emerging global collaboration to investigate immunotherapeutic strategies in HIV-infected children. J. Virus Erad. 1 (3), 134–139.

Perelson, A.S., 2002. Modelling viral and immune system dynamics. Nat. Rev. Immunol. 2 (1), 28–36.

Perelson, A.S., Neumann, A.U., Markowitz, M., Leonard, J.M., Ho, D.D., 1996. HIV-1 dynamics in vivo: Virion clearance rate, infected cell life-span, and viral generation time. Science 271 (5255), 1582–1586.

Ribeiro, R.M., Hazenberg, M.D., Perelson, A.S., Davenport, M.P., 2006. Naïve and memory cell turnover as drivers of CCR5-to-CXCR4 tropism switch in human immunodeficiency virus type 1: Implications for therapy. J. Virol. 80 (2), 802–809.

Ribeiro, R.M., Qin, L., Chavez, L.L., Li, D., Self, S.G., Perelson, A.S., 2010. Estimation of the initial viral growth rate and basic reproductive number during acute HIV-1 infection. J. Virol. 84 (12), 6096–6102.

Richardson, B.A., Mbori-Ngacha, D., Lavreys, L., John-Stewart, G.C., Nduati, R., Panteleeff, D.D., Emery, S., Kreiss, J.K., Overbaugh, J., 2003. Comparison of human immunodeficiency virus type 1 viral loads in Kenyan women, men, and infants during primary and early infection. J. Virol. 77 (12), 7120–7123.

Schmitz, J.E., Kuroda, M.J., Santra, S., Sasseville, V.G., Simon, M.A., Lifton, M.A., Racz, P., Tenner-Racz, K., Dalesandro, M., Scallon, B.J., Ghrayeb, J., Forman, M.A., Montefiori, D.C., Peter Rieber, E., Letvin, N.L., Reimann, K.A., 1999. Control of viremia in simian immunodeficiency virus infection by CD8+ lymphocytes. Science 283 (5403), 857–860.

Shearer, W.T., Quinn, T.C., Larussa, P., Lew, J.F., Mofenson, L., Almy, S., Rich, K., Handelsman, E., Diaz, C., Pagano, M., Smeriglio, V., Kalish, L.A., 1997. Viral load and disease progression in infants infected with human immunodeficiency virus type 1. N. Engl. J. Med. 336 (19), 1337–1342.

Soetaert, K., Petzoldt, T., 2010. Inverse modelling, sensitivity and monte carlo analysis in R using package FME. J. Stat. Softw. 33 (3), 1–28.

Stafford, M.A., Coreya, L., Caob, Y., Daar " ", E.S., Hob, D.D., Perelson, A.S., 2000. Modeling plasma virus concentration during primary HIV infection. J. Theoret. Biol. 203, 285–301.

Tobin, N.H., Aldrovandi, G.M., 2013. Immunology of pediatric HIV infection. Immunol. Rev. 254 (1), 143–169.

van Dorp, C.H., van Boven, M., Boer, R.j.D., 2020. Modeling the immunological pre-adaptation of HIV-1. BioRxiv 2020.01.08.897983.

Wei, X., Ghosh, S.K., Taylor, M.E., Johnson, V.A., Emini, E.A., Deutsch, P., Lifson, J.D., Bonhoeffer, S., Nowak, M.A., Hahn, B.H., Saag, M.S., Shaw, G.M., 1995. Viral dynamics in human immunodeficiency virus type 1 infection. Nature 373 (6510), 117–122.